LJMU Research Online

Chai, Z, Zhang, WD, Degraeve, R, Clima, S, Hatem, F, Zhang, JF, Freitas, P, Marsland, J, Fantini, A, Garbin, D, Goux, L and Kar, GS

 Dependence of switching probability on operation conditions in GexSe1-x ovonic threshold switching selectors

http://researchonline.ljmu.ac.uk/id/eprint/10940/

Article

For more information please contact researchonline@ljmu.ac.uk

Dependence of switching probability on operation conditions in Ge_xSe_{1-x} ovonic threshold switching selectors

Zheng Chai, Weidong Zhang, Robin Degraeve, Sergiu Clima, Firas Hatem, Jian Fu Zhang, Pedro Freitas, John Marsland, Andrea Fantini, Daniele Garbin, Ludovic Goux, and Gouri Sankar Kar

***Abstract*— Ovonic threshold switching (OTS) selector is a promising candidate to suppress the sneak current paths in resistive switching memory (RRAM) arrays. Variations in the threshold voltage (V_{th}), and the hold voltage (V_{hd}) have been reported, but a quantitative analysis of the switching probability dependence on the OTS operation conditions is still missing. A novel characterization method is developed in this work, and the time-to-switch-on/off (t_{on}/t_{off}) at a constant V_{OTS} is found following the Weibull distribution, based on which the dependence of switching probability on pulse bias and time can be extracted and extrapolated, and the switching probability can be ensured with appropriately chosen operation conditions. The difference between square and triangle switching pulses is also explained. This provides a practical guidance for predicting the switching probability under different operation conditions and for designing reliable one-selector-one-RRAM (1S1R) arrays.**

Index Terms—RRAM, selector, OTS, GeSe, probability

I. Introduction

SELECTOR devices are critical in resistive-switching random-access memory (RRAM) arrays for suppressing the sneak path currents that limit the maximum size and reliability of the RRAM array, as shown in **Fig.1a** [1]. Ovonic threshold switching (OTS) chalcogenide material (such as Ge_xSe_{1-x}) based selectors have gained increasing attention because of their high on-state drive current (> 10 MA/cm^2), good half-bias non-linearity, fast switching speed, and excellent endurance, compared with other selectors [2-8].

As shown in **Fig.1b**, when the applied voltage across an OTS device (V_{OTS}) increases, the leakage current at off-state remains very low. As V_{OTS} reaches a critical threshold voltage (V_{th}), the device rapidly switches to the on-state that exhibits a small on-resistance less than 1k ohm [2]. The device remains at the on-state when V_{OTS} is above a critical hold voltage (V_{hd}), below which the current is reduced rapidly and device is reversed back to the off-state. It is always desirable that OTS operation voltages match that of RRAM to enable the one-selector-one-RRAM (1S1R) operation, and the OTS switching time is also expected to match that of RRAMs, which can be in the order of nanoseconds [9]. The statistical analysis of the OTS switching

voltage and switching time and their correlation is therefore critically important for choosing suitable operation conditions for the 1S1R structure. Despite recent efforts in tuning the material composition and process to improve the performance [10-15], an experimental characterization method is still lacking for quantitatively evaluating the switching probability and its dependence on the operation conditions, which is the essential information required for designing the 1S1R array.

In this work, we report a novel method to record the switch-on and -off events either at a constant bias or during the rise/fall pulse edges. It is observed that the time-to-switch-on/-off (t_{on}/t_{off}) at a constant bias follow the Weibull distribution, and V_{th} and V_{hd} measured on the pulse edge follow the normal distribution. In both cases, the statistical switching probability is found dependent on both the pulse bias and time. The operation conditions that ensure a switching probability of 99.7%, equivalent to the 3σ of a normal distribution, can be extracted through extrapolation. This provides a guidance for predicting and choosing switching conditions for reliable 1S1R operations.
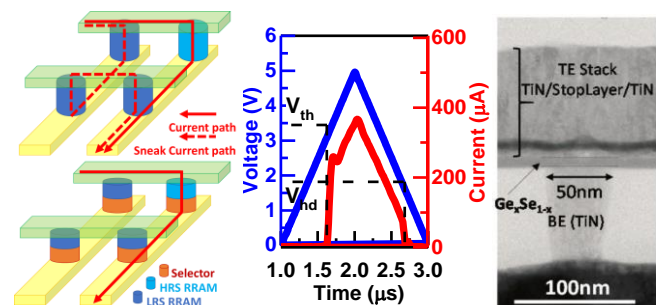

Fig.1. (a) Schematic of selector-embedded 1S1R array for suppressing the sneak current path; (b) A typical I-V of a triangular switching pulse. (c) TEM of the OTS selector used in this work.

II. DEVICE AND CHARACTERIZATION

Amorphous Ge_xSe_{1-x} films are prepared by room temperature physical vapor deposition (PVD). TiN/GeSe/TiN selector devices were integrated in a 300 mm process flow, using a pillar (TiN) bottom electrode which defines the device size down to 50 nm. A Ge_xSe_{1-x} chalcogenide films control from 20 nm down to 5 nm thickness was achieved and passivated with a low-

Zheng Chai, Weidong Zhang, Firas Hatem, Jian Fu Zhang, Pedro Freitas and John Marsland are with the Department of Electronics and Electrical Engineering, Liverpool John Moores University, L3 3AF Liverpool, U.K. (e-mail: w.zhang@ljmu.ac.uk).

Robin Degraeve, Sergiu Clima, Andrea Fantini, Daniele Garbin, Ludovic Goux, and Gouri Sankar Kar are with the Memory Department, imec, 3001 Leuven, Belgium.

Color versions of one or more of the figures in this letter are available online at http://ieeexplore.ieee.org. Digital Object Identifier XXXX

temperature BEOL process scheme, as shown in **Fig.1c**. Three different waveforms have been developed in this work: (1) A triangle pulse to record the I-V, V_{th} and V_{hd} during switching, as shown in **Fig. 1b**. (2) A constant bias square pulse to record the time-to-switch-on, as shown in **Fig. 2a**. (3) A more complex waveform consisting a triangular segment to firstly switch on the device, followed by a constant bias segment to record the switch-off events, as shown in **Fig. 2c**. In this work, the device size is 65 nm, the Ge_xSe_{1-x} thickness is 10 nm and x = 0.4. The fast I-V characterization in this work is carried out with a Keysight B1530A Waveform Generator/Fast Measurement Unit (WGFMU) embedded in a B1500A semiconductor analyzer.

III. RESULTS AND DISCUSSIONS

Square pulses are usually used to program the RRAM and selector devices. In **Fig. 2b, d**, an OTS device is switched on and off by a square pulse for 100 cycles and the I-t waveforms are measured and plotted together. It is observed that the time-to- switch-on (t_{on}) recorded at the constant pulse top bias of 2.8 V spreads over a wide time range. In some cycles, the device is already switched-on on the rising edge before the bias reached 2.8V; in many cycles the device is switched-on at 2.8 V with various t_{on} during the pulse; and in other cases, the device has not switched on till the end of the pulse. It is found that t_{on} follows the Weibull distribution, as shown in **Fig. 3a**. The switch-on events occurred on the rising edge and those beyond the pulse duration cannot be measured accurately due to the limitation of B1530A's measurement resolution. By following the Weibull distribution, however, these data points can be extrapolated using the Weibull plot, as also shown in **Fig.3a**. It is found that t_{on} spreads over 5 orders of magnitude.

The t_{on} / t_{off} distribution are examined by the Weibull plot which is widely used in industries and can be described as,

$$\ln(-\ln(1 - F(x))) = k\ln x - k\ln\lambda \qquad (1)$$

where F(x) is the empirical cumulative distribution function, λ is the scale parameter and *k* is the shape parameter [16, 17].

It is also observed that there is a consistent trend that the t_{on} gradually decreases as V_{OTS} increases, as shown in **Fig.3a**. t_{on} at different biases follows the Weibull distribution with the same slope, shifting towards shorter t_{on} at higher V_{OTS}. The dependence of t_{on} on V_{OTS} is clearly shown in **Fig. 3b**. A 99.7% switching-on probability, equivalent to the 3σ of the normal distribution ($t_{on,3\sigma}$), can be obtained via a linear extrapolation. The pulse duration that ensure this switch-on probability decreases linearly against bias in the log-linear scale. An increase of bias by 0.2V will lead to a $t_{on,99.7\%}$ decrease by nearly two orders. V_{OTS} of 3.5 V is needed in order to achieve a t_{on} of 10 ns with 99.7% of probability by a linear extrapolation.

Similarly, the switch-off process follows the same trend but in the opposite direction, as shown in **Fig. 4**. A lower V_{OTS} leads to a shorter time to switch off the device, and t_{off} also follows the Weibull distribution, spreading over a range of 4 orders of magnitude with a steeper slope than that of t_{on}. The dependence of t_{off} on V_{off} is clearly shown in **Fig. 4b**, in which the pulse duration that ensures a 99.7% switching-off probability decreases linearly when the bias decreases in the log-linear

scale. A decrease of bias by 0.2 V will lead to a $t_{off,99.7\%}$ decrease of more than 4 orders. V_{off} of 1.5 V is already sufficient to achieve a t_{off} of 10 ns with 99.7% of probability. Since the bottom bias of a square pulse, V_{off}, is normally 0 V, much lower than 1.5 V, the extrapolated $t_{off,99.7\%}$ at 0 V is much shorter than 1 ps, therefore the switch-off is a much faster process than switch-on. The statistical distribution of t_{off} observed in Fig.4 is not a concern for OTS operations.
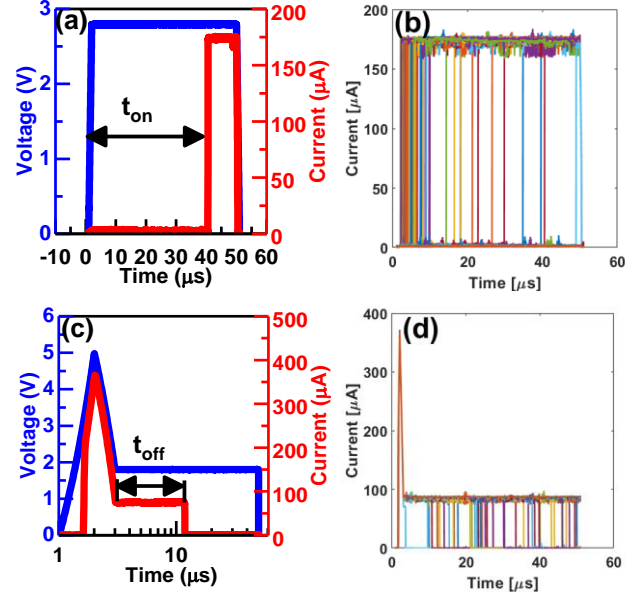

Fig. 2. (a) t_{on} measurement waveform; (b) Typical I-t waveforms of switch-on events at 2.8 V during 100 cycles; (c) t_{off} measurement waveform; (d) Typical I-t waveforms of switch-off events at 1.9 V during 100 cycles. The duration of all constant biases is 50 µs. The rise/fall time is 1 µs for both the triangle and square pulses. The triangle pulse amplitude is 5 V. The sampling time of the current measurement is 10 ns/point.
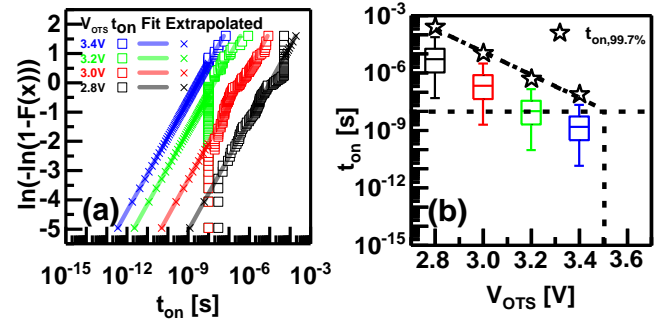

Fig. 3. (a) Weibull plot of measured data (□), linear fitting (——) and extrapolation beyond measurement resolution and pulse duration (✕) of t_{on} at different biases. (b) Boxplot of t_{on} at different biases and the extracted t_{on} to ensure the probability of switching-on reaches 99.7% (☆) as obtained from the Weibull distribution. V_{OTS} of 3.5 V is needed to achieve a t_{on} of 10 ns with 99.7% of probability by a linear extrapolation.

Triangular pulses are also commonly used to monitor the volatile switching in time domain for OTS selectors, as it enables the incremental I-V measurement in both forward and backward sweeps [3]. The impact of rise/fall time of the triangular pulse on V_{th} and V_{hd} is investigated in this work by switching the device with varying rise/fall times in a sequence of 1 µs, 10 µs, 100 µs, 1 ms and then 1 µs again. For each

rise/fall time, the device is cycled 100 times. It is observed in **Fig. 5a&b** that, as $t_{rise/fall}$ increases from 1 µs to 1 ms, the V_{th} decreases while V_{hd} increases. In the last 1 µs test, both the V_{th} and V_{hd} agree well with those in the first 1 µs test, supporting that there is negligible degradation during the cycling and the V_{th} decrease and V_{hd} increase are caused by slower rise/fall speed.
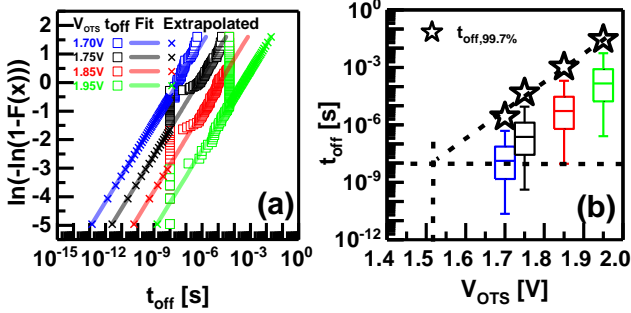

Fig. 4. (a) Weibull plot of measured data (□), linear fitting (——) and extrapolation beyond measurement resolution and pulse duration (✗) of t_{off} at different biases (b) Boxplot of t_{off} at different biases and extracted t_{off} to ensure the probability of switching-off reaches 99.7% as obtained from the Weibull distribution (☆). V_{OTS} of 1.5 V is needed in order to achieve a t_{off} of 10 ns with 99.7% of probability by a linear extrapolation.
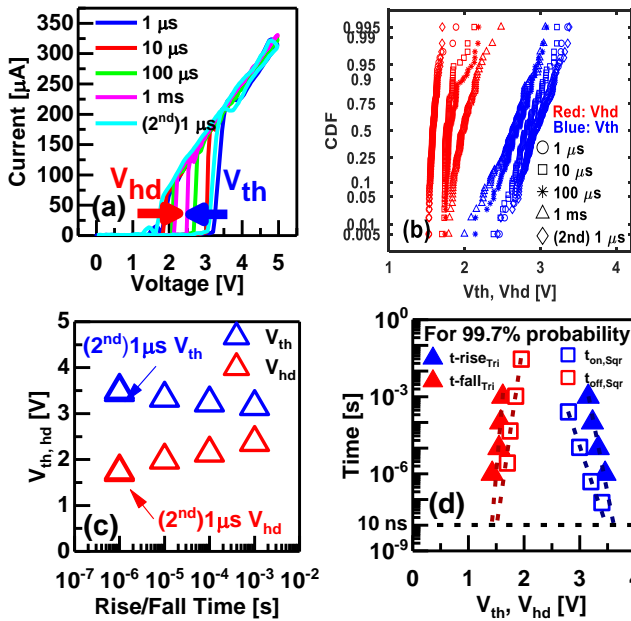

Fig. 5. (a) Demonstration of the I-V with different ramp rates; (b) CDF of the statistical V_{th} and V_{hd} distribution out of 100 switching cycles with different rise/fall time follow the normal distribution; (c) The extrapolated V_{th} and V_{hd} to ensure 99.7% probability in triangular waveform; (d) Comparison of V-t trade-off in triangular waveform and square waveforms, to ensure 99.7% switching probability.

The distribution and the extracted 3σ value of V_{th} and V_{hd} are shown in **Fig. 5b** and **5c** and the trend agrees with that of the square pulse obtained in **Fig. 3b&4b**. A comparison between the t_{on}/t_{off} of square pulses and t_{rise}/t_{fall} of triangular pulses in **Fig. 5d** shows a reasonably good agreement at shorter times. The larger deviation at slower triangular edges can be explained as follows. Since the switching on and off are predominantly controlled by the bias and its duration within the $V\sim V_{th}$ and $V\sim V_{hd}$ range, respectively. For slower triangle sweeps, a longer

part of the edge time, which is below $V\sim V_{th}$ for switching-on and above $V\sim V_{hd}$ for switching-off, respectively, has negligible impact, and its actual switching time is much shorter. Hence, it needs a larger bias for switching-on and a smaller bias for switching-off in order to achieve the same switching time as the corresponding square pulse shown in **Fig. 5d**. This supports that the t_{on}/t_{off} measurement at constant biases is a reliable method to evaluate the operation conditions.

The stochastic Weibull distribution of t_{on}/t_{off} and the trade-off between the bias and time can be explained by the conductive filament formation/deformation during switch-on/off [8]. The extrapolations toward the switching speed at 10 ns with 99.7% switching probability agree reasonably well for both pulse waveforms. Switch-off is a much faster process, so that t_{off} is not a concern for OTS operations. On the other hand, it is critical to meet the switch-on voltage and time conditions based on the statistical analysis presented in this work in order to ensure the switching probability of OTS selector.

IV. CONCLUSIONS

A novel method is presented in this work, for the first time, to evaluate the dependence of switching probability on the operation conditions in Ge_xSe_{1-x} OTS selectors. The time-to-switch-on/-off at a constant bias follow Weibull distribution, and V_{th} and V_{hd} measured on the pulse edge follow normal distribution. The statistical switching probability is found dependent on both the bias and time. The operation conditions that ensure a switching probability of 99.7%, equivalent to the 3σ of a normal distribution, can be extracted through extrapolation, providing a guidance for predicting and choosing switching conditions for reliable 1S1R operations.

Reference

[1] L. Zhang, B. Govoreanu, A. Redolfi, D. Crotti, H. Hody, V. Paraschiv, S. Cosemans, C. Adelmann, T. Witters, S. Clima, Y.Y. Chen, P. Hendrickx, D.J. Wouters, G. Groeseneken, M. Jurczak, High-drive current (>1MA/cm²) and highly nonlinear (>10³) TiN/amorphous-Silicon/TiN scalable bidirectional selector with excellent reliability and its variability impact on the 1S1R array performance, *in IEDM Tech. Dig.,* Dec. 2014, pp. 6.8.1-6.8.4 DOI:10.1109/IEDM.2014.7047000

[2] S.R. Ovshinsky, Reversible Electrical Switching Phenomena in Disordered Structures, *Phys. Rev. Lett., vol.* 21, no. 20-11 p. 1450, Nov. 1968, DOI:https://doi.org/10.1103/PhysRevLett.21.1450

[3] B. Govoreanu, G.L. Donadio, K. Opsomer, W. Devulder, V.V. Afanas'ev, T. Witters, S. Clima, N.S. Avasarala, A. Redolfi, S. Kundu, O. Richard, D. Tsvetanova, G. Pourtois, C. Detavemie, L. Goux, G.S. Kar, Thermally stable integrated Se-based OTS selectors with >20 MA/cm² current drive, >3.10³ half-bias nonlinearity, tunable threshold voltage and excellent endurance, *in VLSI Symp. Tech. Dig.,* Jun. 2017 DOI:10.23919/VLSIT.2017.7998207

[4] N.S. Avasarala, G.L. Donadio, T. Witters, K. Opsomer, B. Govoreanu, A. Fantini, S. Clima, H. Oh, S. Kundu, W. Devulder, M. H. van der Veen, J. Van Houdt, M. Heyns, L. Goux, G.S. Kar, Half-threshold bias Ioff reduction down to nA range of thermally and electrically stable high-performance integrated OTS selector, obtained by Se enrichment and N-doping of thin GeSe layers, *in VLSI Symp. Tech. Dig.,* Jun. 2018 DOI: 10.1109/VLSIT.2018.8510680

[5] J. Song, J. Woo, A. Prakash, D. Lee, and H. Hwang, Threshold selector with high selectivity and steep slope for cross-point memory array, *IEEE Electron Device Lett., vol.* 36, no. 7, pp. 681–683, May 2015 DOI: 10.1109/LED.2015.2430332

[6] W. Chen, H. J. Barnaby, and M.N. Kozicki, Volatile and nonvolatile switching in Cu-SiO₂ programmable metallization cells, *IEEE Electron*

Device Lett., vol. 37, no. 5, pp. 580–583, Mar. 2016, DOI: 10.1109/LED.2016.2540361

[7] M. Son, J. Lee, J. Park, J. Shin, G. Choi, S. Jung, W. Lee, S. Kim, S. Park, and H. Hwang, Excellent Selector Characteristics of Nanoscale VO$_2$ for High-Density Bipolar ReRAM Applications, *IEEE Electron Device Lett.* vol. 32, no. 11, pp. 1579–1581, Aug. 2011 DOI: 10.1109/LED.2011.2163697

[8] S. Clima, B. Govoreanu, K. Opsomer, A. Velea, N. S. Avasarala, W. Devulder, I. Shlyakhov, G. L. Donadio, T. Witters, S. Kundu, L. Goux, V. Afanasiev, G. S. Kar and G. Pourtois, Atomistic Investigation of the Electronic Structure, Thermal Properties and Conduction Defects in Ge-rich GexSe1-x Materials for Selector Applications, in IEDM Tech. Dig., Dec. 2017, pp. 4.1.1- 4.1.4 DOI: 10.1109/IEDM.2017.8268323

[9] B. Govoreanu, G.S. Kar, Y.Y. Chen, V. Paraschiv, S. Kubicek, A. Fantini, I.P. Radu, L. Goux, S. Clima, R. Degraeve, N. Jossart, O. Richard, T. Vandeweyer, K. Seo, P. Hendrickx, G. Pourtois, H. Bender, L. Altimime, D.J. Wouters, J.A. Kittl, M. Jurczak, 10×10nm^2 Hf/HfOx crossbar resistive RAM with excellent performance, reliability and low-energy operation, *in IEDM Tech. Dig.,* Dec. 2011, DOI:10.1109/IEDM.2011.6131652

[10] R. Aluguri and T.-Y. Tseng, Overview of Selector Devices for 3-D Stackable Cross Point RRAM Arrays, *IEEE J. Electron Devices Soc.,* vol. 4, no. 5, 2016 DOI: 10.1109/JEDS.2016.2594190

[11] H.Y. Cheng, W.T.C. Chien, I. Kuo, E.F.K. Lai, Y. Zhu, J.L. Jordan-Sweet, A. Ray, F. Carta, F.M. Lee, P.H. Tseng, M.H. Lee, Y.Y. Lin, W. Kim, R. Bruce, C.W. Yeh, C.H. Yang, M.J. BrightSky, H.L. Lung, An ultra high endurance and thermally stable selector based on TeAsGeSiSe chalcogenides compatible with BEOL IC Integration for cross-point PCM, *in IEDM Tech. Dig.,* Dec. 2017, DOI: 10.1109/IEDM.2017.8268310

[12] S.-Y. Shin, J. M. Choi, J. Seo, H.-W. Ahn, Y. G. Choi, B.-k. Cheong, S. Lee, The effect of doping Sb on the electronic structure and the device characteristics of Ovonic Threshold Switches based on Ge-Se, *Sci. Rep., vol.* 4, no. 7099, Nov. 2014 DOI: 10.1038/srep07099.

[13] M.-J. Lee, D. Lee, H. Kim, H.-S. Choi, J.-B. Park, H.G. Kim, Y.-K. Cha, U.-I. Chung, I.-K. Yoo, K. Kim, Highly-scalable threshold switching select device based on chaclogenide glasses for 3D nanoscaled memory arrays, *in IEDM Tech. Dig.,* Dec. 2012 DOI: 10.1109/IEDM.2012.6478966

[14] S.A. Chekol, J. Yoo, J. Park, J. Song, C. Sung, H. Hwang, A C–Te-based binary OTS device exhibiting excellent performance and high thermal stability for selector application, *Nanotechnology,* vol. 29, no. 34, p. 345202, Jun. 2018 DOI: 10.1088/1361-6528/aac9f5

[15] Y. Koo, K. Baek, H. Hwang, Te-based amorphous binary OTS device with excellent selector characteristics for x-point memory applications, *in VLSI Symp. Tech. Dig.,* Jun. 2016 DOI: 10.1109/VLSIT.2016.7573389

[16] W. Weibull, A Statistical Distribution Function of Wide Applicability, Journal of Applied Mechanics, vol. 18, pp. 293-297, September 1951.

[17] E. Wu, B. Li, J. H. Stathis, R. Achanta, R. Filippi, and P. McLaughlin, "A time-dependent clustering model for non-uniform dielectric breakdown," *in IEDM Tech. Dig.,* 2013, pp. 15.13.1-15.13.4. DOI: 10.1109/IEDM.2013.6724635